RESEARCH ARTICLE | JUNE 12 2026

Persistent homology as efficient phase descriptor for 2D skyrmion lattices

Michiki Taniwaki ; Thomas Brian Winkler ; Jan Rothörl ; Raphael Gruber ; Chiharu Mitsumata ; Masato Kotsugi ; Mathias Kläui

APL Mach. Learn. 4, 026111 (2026)
https://doi.org/10.1063/5.0331214

Persistent homology as efficient phase descriptor for 2D skyrmion lattices

Cite as: APL Mach. Learn. 4, 026111 (2026); doi: 10.1063/5.0331214
Submitted: 24 February 2026 • Accepted: 20 May 2026 •
Published Online: 12 June 2026

Michiki Taniwaki,[1,2] Thomas Brian Winkler,[2,3] Jan Rothörl,[2] Raphael Gruber,[2] Chiharu Mitsumata,[4] Masato Kotsugi,[1] and Mathias Kläui[2,a)]

AFFILIATIONS

[1] Department of Materials Science and Technology, Tokyo University of Science, Niijuku 125-8585, Japan
[2] Institute of Physics, Johannes Gutenberg University Mainz, 55099 Mainz, Germany
[3] Institute of Molecules and Materials, Radboud University, Heyendaalseweg 135, 6525AJ Nijmegen, The Netherlands
[4] Graduate School of Pure and Applied Sciences, University of Tsukuba, Tenodai 305-8571, Japan

[a)] **Author to whom correspondence should be addressed:** klaeui@uni-mainz.de

ABSTRACT

Two-dimensional (2D) particle systems, such as magnetic skyrmions, exhibit topological phase transitions between unique 2D phases. However, a simple and computationally efficient methodology to capture lattice configurational properties and construct an appropriate, easily calculable indicator for phase identification remains elusive. Here, we propose an indicator for topological phase transitions using persistent homology (PH). PH provides a complementary topological description by capturing persistent features derived from the configurational properties of the lattice. The proposed persistent-homology-based indicator, which selectively counts stable features in a persistence diagram, effectively traces the lattice's ordering changes, as confirmed by comparisons with the conventionally used measure of the ordering (the magnitude of the orientational order parameter $\langle|\Psi_6|\rangle$), typically used to identify lattice phases. We demonstrate the applicability of our indicator to experimental data, showing that it yields results consistent with those of simulations. This experimental validation highlights the robustness of the proposed method for real physical systems beyond idealized simulated systems. While our method is demonstrated in the context of skyrmion lattice systems, the approach is general and can be extended to other two-dimensional systems composed of interacting particles. The proposed topological indicator remains computationally tractable for the system sizes considered here, while preserving the topological invariant-based structural information.

INTRODUCTION

Magnetic skyrmions are chiral, vortex-like spin textures characterized by topologically enhanced stability,[1,2] often treated as quasiparticles due to their particle-like behavior.[3,4] These structures have garnered significant attention from researchers for their energy-efficient manipulation via spin-transfer and spin–orbit torques,[5] offering promising pathways toward next-generation information storage and unconventional computing devices.[6] A possible application of skyrmions is the racetrack memory as a high-density memory technology.[7–9] Such future skyrmionic applications are based on the behavior of multiple skyrmions. It is, therefore, important to investigate their physical properties and their collective arrangements to achieve such technological applications using skyrmions. From a fundamental physics perspective, ensembles of skyrmions, known as skyrmion lattices, can exhibit complex phase behavior, including two-dimensional melting transitions.[10] These transitions are theoretically captured by the Kosterlitz–Thouless–Halperin–Nelson–Young (KTHNY) framework, which describes the emergence of intermediate hexatic phases and the role of topological defects, such as dislocations and disclinations.[10] Although this behavior has been extensively studied in colloidal systems, skyrmion lattices offer distinct advantages due to their tunability and controllable dynamics that can be fully captured in real time and real space, making them an ideal platform for investigating two-dimensional phase transitions.[11]

Despite intensive research, topology-based descriptors of lattice configurations remain much less explored than conventional bond-orientational measures. Conventional methods, such as the local orientational order parameter $\psi_6(r)$ and the orientational correlation function, provide well-established local and spatially resolved descriptions of sixfold order.[5,11–13] In the present work, we use the averaged absolute value $\langle|\Psi_6|\rangle$ as a conventional scalar reference quantity and investigate whether a complementary topology-based descriptor can consistently track ordering changes from a different, multi-scale geometric perspective.

To address this, we introduce a framework based on Topological Data Analysis (TDA), a concept from algebraic topology used to analyze the geometric structure of objects, specifically applying Persistent Homology (PH) to extract the configurational properties of lattice configurations.[14–19] The PH provides a multi-scale view of topological features by analyzing how connected components and loops emerge and disappear across a filtration. This approach has seen successful applications in biological and materials systems.[20–24] PH can capture and describe the microscopic processes involved in the phase transitions.[16] In this work, we apply PH in a particle-based approach, which models skyrmions as interacting quasiparticles and focuses on their positional configuration that does not require knowledge of the full spin texture. This abstraction enables an efficient computational treatment and highlights the essential geometric features responsible for phase behavior.[3,4,25] We propose a topological indicator,[26,27] the Persistent Generator Count with Relative Stability (PGCRS), which selectively counts only the robust topological features of the persistent diagram (PD) in each homology dimension, generated by PH. PGCRS reliably detects phase transitions in the lattice, correlates with conventional measures, and offers a significantly reduced computational complexity. A distinctive aspect of our approach is inverse analysis,[28] to trace persistent generators back to specific real-space configurations, enabling a direct physical interpretation of the microscopic structures responsible for topological phase behavior. This shift from scalar reductions of local order to counting persistent topological features offers a complementary perspective for understanding 2D phase transitions. We apply our framework to experimentally acquired skyrmion configurations, demonstrating the practical applicability of our method for real physical systems. While the focus of this work is on skyrmion systems, the underlying method can be extended to other two-dimensional quasiparticle systems.

METHODS

In this work, we treat skyrmions as quasiparticles without considering their detailed spin textures, following previous studies.[3,25,29] This abstraction allows us to focus on the configurational properties relevant to phase transitions while significantly simplifying the computational analysis. We apply PH analysis to experimental skyrmion configurations, as the numerically simulated results are provided in the supplementary material.

In the subsequent sections, we first describe the experimental setup, then introduce the persistent homology analysis, and present the PH-based indicator. Finally, we describe the conventionally used measure of the ordering.

Experimental skyrmion lattices

The experimental skyrmion configuration data used in this work are obtained from magnetic multilayer stacks: Ta(5)/$Co_{20}Fe_{60}B_{20}$(0.9)/Ta(0.07)/MgO(2)/Ta(5).[3,11] The experimental states analyzed below are taken from the hexagonally confined skyrmion system reported in Ref. 11. While some order has been observed in unconfined systems, pinning effects can suppress long-range order in such systems.[5,13,30] By contrast, control over the order is much easier in confined geometries, which help stabilize the lattice.[11,31] Magnetic fields are applied both in-plane (IP) and out-of-plane (OOP) using an evico magnetics GmbH Kerr microscope, with the sample maintained at a constant temperature of 333.5 K. Skyrmions are nucleated by applying an IP field pulse under a constant OOP field. The lattice is subsequently equilibrated using an oscillating OOP field at 100 Hz (with amplitudes up to 60 μT), combined with a constant OOP offset field.[11,30] The skyrmion size is precisely controlled via the applied OOP magnetic field. The magnetic field conditions are varied every 62.5 s (corresponding to every 1000 frames) to gather sufficient statistics for analyzing the topological phases. The positions of individual skyrmions are identified using a machine-learning-based, pixel-wise classification algorithm.[32] In the present work, the PH analysis is applied to the point cloud formed by the detected skyrmion centers. In this formulation, the method does not require skyrmions to be circular, touching, or arranged in an ideal hexagonal environment. Rather, it uses the connectivity and loop structure of the detected positions across scales. This makes the approach naturally applicable to distorted, dilute, confined, or partially isolated configurations, although explicit use of skyrmion size or shape information is beyond the scope of the present study. The detailed analysis procedure can be found in Ref. 11.

Persistent homology for two-dimensional coordinates of quasiparticles

In the persistent homology analysis, an alpha-filtration of the zeroth- and first-degree homology is often applied to the two-dimensional coordinates of quasiparticles.[14,33,34] From this, the corresponding persistence diagrams (PD0 and PD1) can be generated.[14] The inverse analysis method of persistent homology is applied to the selected frames of our data, which can identify the original structure corresponding to a specific generator in the persistence diagram.[28] Because persistent homology is supported by a mathematical stability theory,[35] small perturbations of the input point cloud are expected, in principle, to induce only small changes in the persistence diagram; accordingly, PGCRS may be less sensitive to moderate coordinate perturbations. This possible robustness is relevant for experimentally obtained skyrmion configurations, where extracted coordinates may be affected by imaging noise, brightness fluctuations, segmentation uncertainty, or approximate assumptions about skyrmion shape; however, the present work does not include a dedicated quantitative comparison of noise sensitivity with ψ_6. The details of the alpha-filtration, PDs, and inverse analysis are described in Figs. 1–3.

Persistent homology-based indicator

To measure the ordering of the system within the PH framework, we define the Persistent Generator Count with Relative Stability (PGCRS), which provides a scalar descriptor of persistent topological features. The PGCRS is defined as

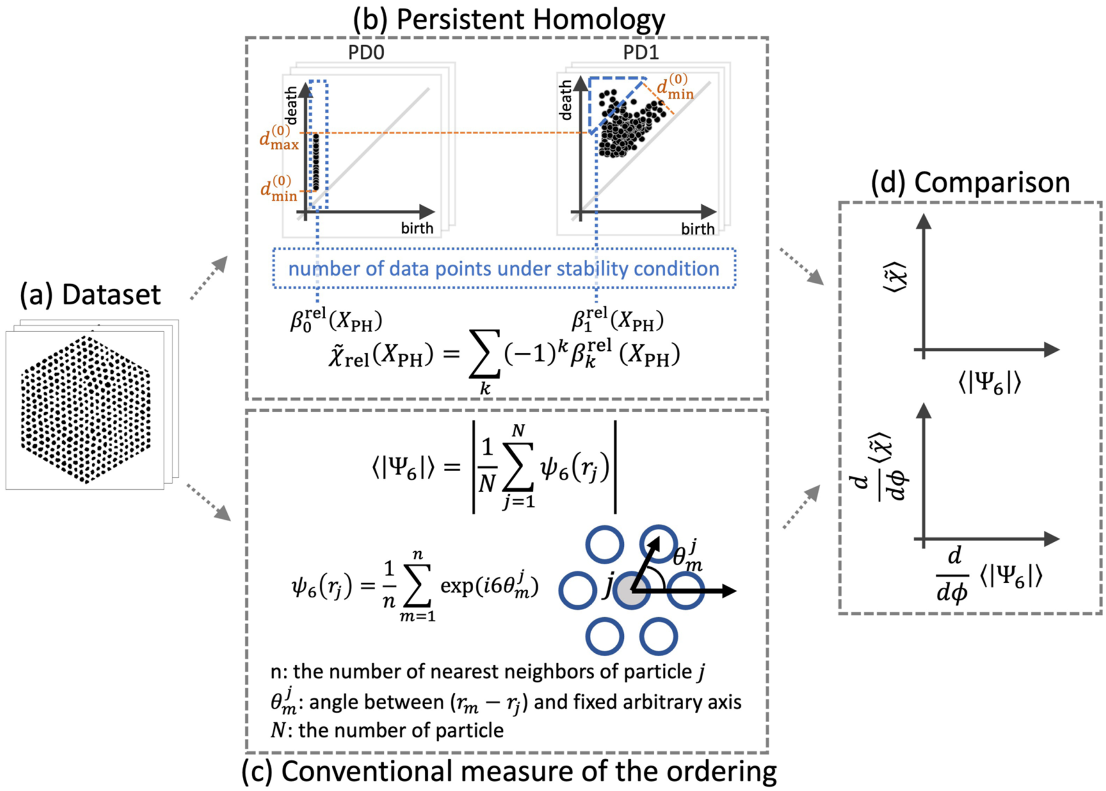

FIG. 1. Schematics of the key concepts and workflow of the persistent homology method used in this study. (a) Skyrmion coordinates, (b) Persistent Homology (PH) analysis, (c) calculation of a conventional lattice-ordering measure, and (d) comparison between the PH-based indicator and the conventional measure.

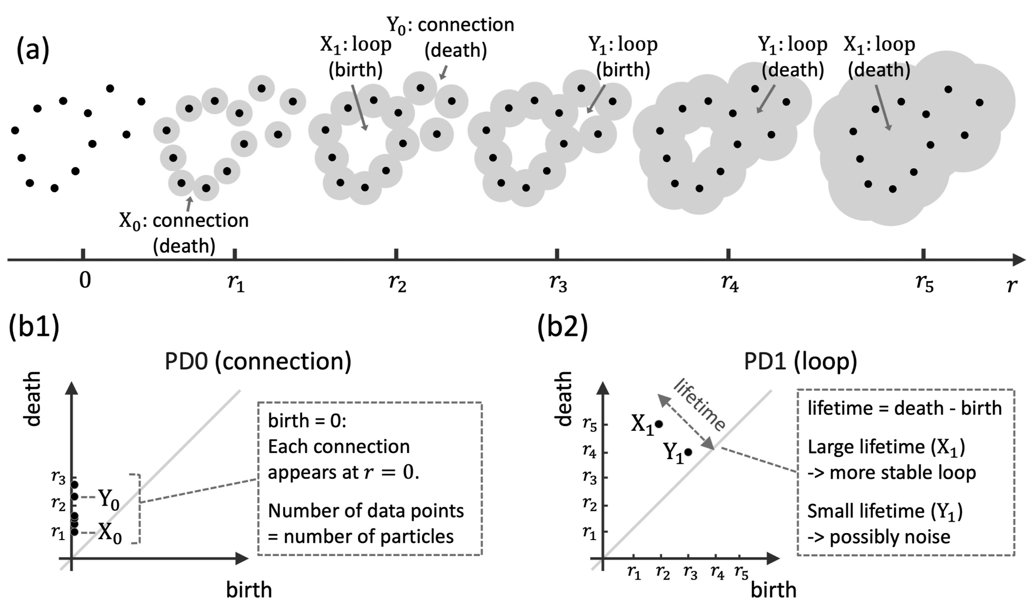

FIG. 2. Schematic illustration of the filtration process and construction of persistence diagrams (PDs). (a) Illustration of the topological features—connected components and loops—emerging during the filtration process, where the radius of disks centered at the skyrmion coordinates is varied. (b1) PD0 (zeroth-degree homology) and (b2) PD1 (first-degree homology) with interpretations. For a detailed explanation of the PH filtration process, please refer to Ref. 15.

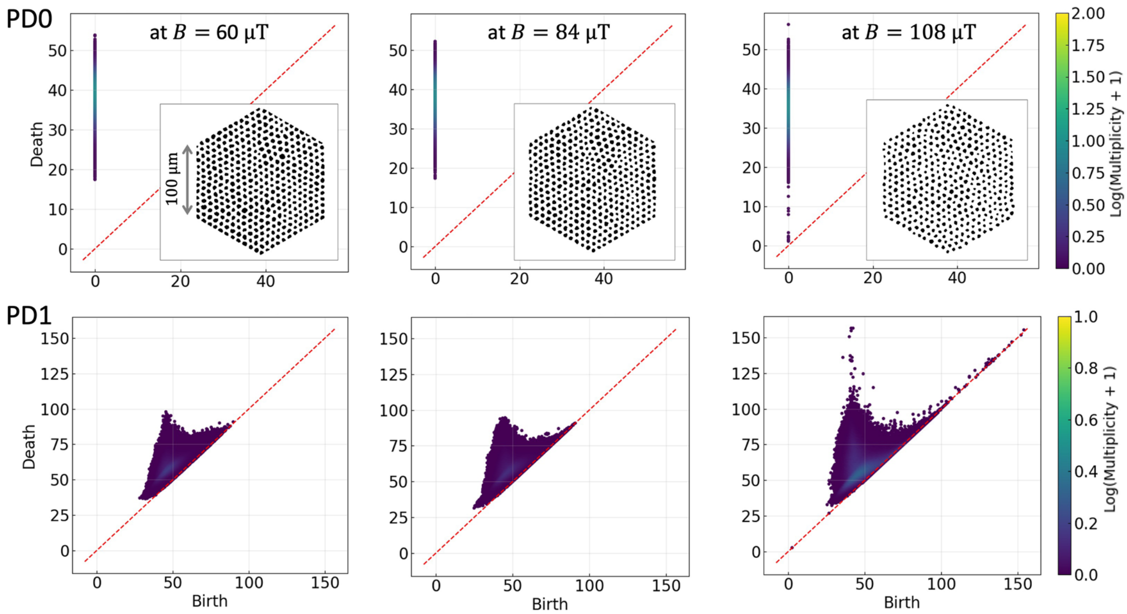

FIG. 3. Phase-dependent evolution of persistence diagrams (PDs) for skyrmion lattices. Average PDs of the zeroth- and first-degree homology, for three states under applied OOP magnetic fields of B = 60, 84, and 108 μT, correspond to solid, hexatic, and liquid phases. These states have previously been identified as solid-, hexatic-, and liquid-like, respectively, by conventional orientational-correlation analysis in the same confined experimental system.[11] The "birth" and "death" represent the filtration parameter values/stages in a filtration process of persistent homology in which topological features emerge and disappear, respectively. The color map represents the multiplicity of generators/data points in the PD. The insets in the zeroth-degree homology PDs display the corresponding real-space configurations, identified using a machine-learning-based, pixel-wise classification algorithm.[32]

$$\tilde{\chi}_{\mathrm{rel}}(X_{\mathrm{PH}}) = \sum_{k} (-1)^k \beta_k^{\mathrm{rel}}(X_{\mathrm{PH}}), \tag{1}$$

where k denotes the homology dimension, X_{PH} denotes the PH-based representation used to construct the indicator, and $\beta_k^{\mathrm{rel}}(X_{\mathrm{PH}})$ denotes the number of data points in the PD that satisfy the stability conditions for the kth homology dimension, as described in Fig. 1 and in the supplementary material. In particular, $k = 0$ corresponds to connected components and $k = 1$ corresponds to loop structures. In this formulation, the PGCRS provides a single integer that summarizes the selected persistent topological features within the corresponding PDs. Although PGCRS is motivated by the Euler characteristic, it is used here as a practical PH-based descriptor rather than as an exact evaluation of the Euler characteristic of a single fixed complex. PGCRS reflects the multi-scale nature of the configuration and the property of a topological invariant, while remaining computationally tractable.[36,37] Further theoretical justification is required to fully elucidate its implications. For detailed discussions of topological invariants and their relation to phase transitions, see Refs. 16, 26, and 27.

Conventionally used measure of ordering

To identify the topological phases, including liquid, hexatic, and solid phases, the following quantities are conventionally used as orientational-order measures.[5,10–13] Among them, the averaged absolute value of the local orientational order parameter, $\langle|\Psi_6|\rangle$, is defined as[5]

$$\langle|\Psi_6|\rangle = \left| \frac{1}{N} \sum_{j=1}^{N} \psi_6(r_j) \right|, \tag{2}$$

where

$$\psi_6(r_j) = \frac{1}{n} \sum_{m=1}^{n} \exp(i6\theta_m^j), \tag{3}$$

n is the number of nearest neighbors of the reference particle j, θ_m^j is the angle between the bond vector $r_m - r_j$ and a fixed arbitrary axis, and N is the total number of particles. The nearest neighbors are determined using a Voronoi tessellation.[38] The factor of 6 in the exponent reflects the sixfold rotational symmetry of a perfect hexagonal lattice. When a particle's six nearest neighbors form an ideal hexagonal arrangement, $|\psi_6| = 1$ is obtained.

This measure provides a convenient scalar summary of local sixfold bond-orientational order and is widely used to compare different system conditions. More generally, $\psi_6(r)$ and the orientational correlation function provide well-established local and spatially resolved descriptions of ordering. In the present work, we use the averaged quantity $\langle|\Psi_6|\rangle$ as a conventional scalar reference for comparison with PGCRS.

RESULTS AND DISCUSSION

To provide an overview of our approach, we summarize the overall analysis pipeline used in this study. Figure 1 presents a schematic overview of the analysis workflow. We first (a) obtain the

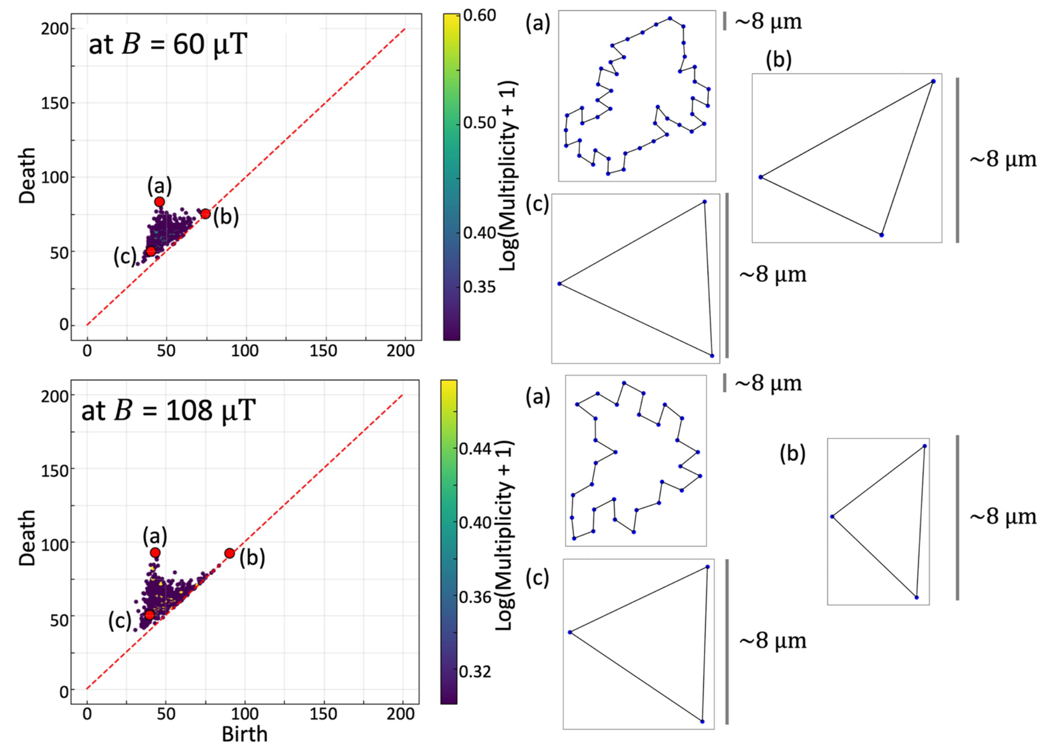

FIG. 4. Real-space interpretation of persistent features. Inverse analysis for the two states at $B = 60$ and $108\ \mu$T traces specific data points in the persistence diagram back to real-space configurations. In each state, the points labeled (a), (b), and (c) correspond to persistent homology generators with a large lifetime (a), a small lifetime and a small birth value (b), and a small lifetime and a large birth value (c).

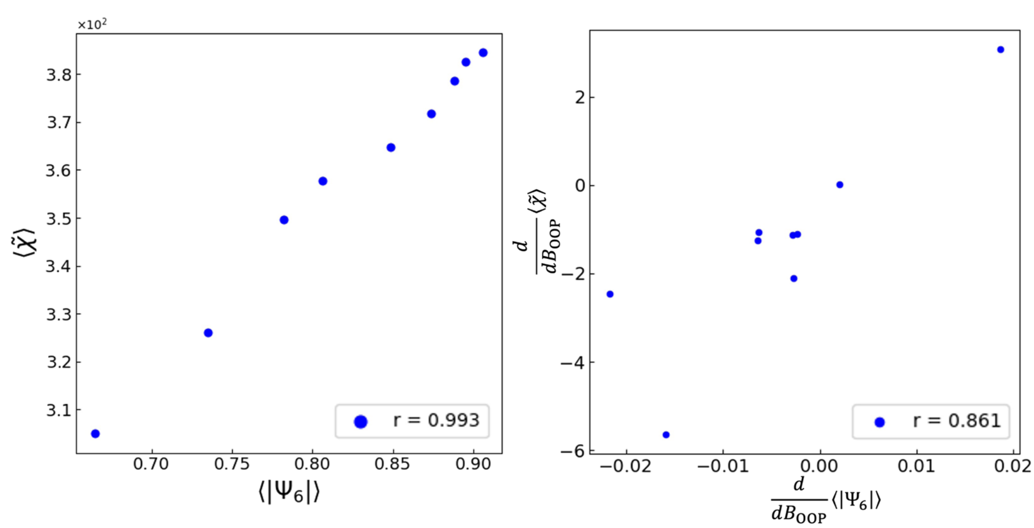

FIG. 5. Comparison between $\langle\tilde{\chi}\rangle$ and $\langle|\Psi_6|\rangle$. Here, $\langle\tilde{\chi}\rangle$ denotes the persistent homology-based measure, and $\langle|\Psi_6|\rangle$ denotes the conventional measure of orientational ordering; the definitions and computational procedures for both are described in the Methods section. Both quantities are evaluated from the experimental skyrmion lattice configurations as a function of the applied out-of-plane magnetic field B_{OOP}. Their first derivatives $\mathrm{d}\langle\tilde{\chi}\rangle/\mathrm{d}B_{\mathrm{OOP}}$ and $\mathrm{d}\langle|\Psi_6|\rangle/\mathrm{d}B_{\mathrm{OOP}}$, are estimated using the Gaussian process regression. A correlation is indicated by the Pearson correlation coefficients of $r = 0.993$ and $r = 0.861$.

coordinates of skyrmions from the experimental data and then (b) apply the PH analysis with (c) the calculation of the conventionally used measure of the ordering. Finally, we (d) compare the two indicators. The experimental procedure is detailed in the Methods section. The PH analysis is described in the following subsections and presented in Figs. 2–4, where the PDs and their interpretation through inverse analysis are provided. Subsequently, the PH-based indicators and the conventionally used measure are compared in terms of consistency and computational cost, as described in Fig. 5. Validation using Molecular Dynamics (MD) simulations is presented in the supplementary material (Figs. S1–S6).

Persistent homology and persistence diagrams for experimental skyrmion lattices

We first illustrate how PH characterizes local and global structural features. Figure 2 illustrates the filtration process and the corresponding persistence diagrams (PDs) for the zeroth- and first-degree homology dimensions. The filtration process is performed by continuously increasing the radius of disks centered at the skyrmion coordinates, thereby tracking the emergence and disappearance of topological features such as connected components and loops. The birth and death values in the PDs correspond to the specific filtration parameter r at which these topological features appear and vanish, respectively. The PD0 diagram captures the birth and death of connected components (zeroth-degree homology), while the PD1 diagram records the birth and death of loop-like structures (first-degree homology). In particular, the data points in PD0 indicate when individual skyrmions (disks) merge; thus, all birth values are zero, and the death values correspond to the connection events. The number of data points in PD0 equals the number of skyrmions in the system. In PD1, the lifetime $(\text{death} - \text{birth})$ represents the persistence of loop-like structures formed by connected skyrmions. A large lifetime indicates robust loops that persist over a wide range of filtration parameters, whereas a small lifetime corresponds to transient loops that quickly disappear as the filtration parameter varies, or possibly to noise. For a detailed explanation of the PH filtration process, please refer to Ref. 15.

We next apply PH analysis to skyrmion lattices measured under different magnetic fields to examine how topological features evolve across phase regimes.

Figure 3 shows the persistence diagrams (PDs) of the zeroth- and first-degree homology obtained from three states of the experimental skyrmion lattice under applied out-of-plane (OOP) magnetic fields of $B = 60$, 84, and 108 μT. These three states were previously characterized in the same confined experimental system by the orientational correlation function $c_6(r)$ as solid-, hexatic-, and liquid-like, respectively.[11] The phase labels used here, therefore, follow the conventional characterization of Ref. 11, rather than being inferred from PH alone. In each PD, the "birth" and "death" values represent the filtration stages during which topological features emerge and disappear, respectively, and the color map indicates the multiplicity of generators. The "birth" and "death" values correspond to the radii of disks grown during the filtration process, as explained in Fig. 2.

The PD0 for the disordered configuration (e.g., $B = 108$ μT) displays a broader distribution compared to the more ordered configuration (e.g., $B = 60$ μT). In addition, the PD1 for the disordered state exhibits a greater number of generators with large lifetimes (i.e., features farther from the diagonal line), while the ordered state tends to show fewer such persistent features. Although the raw PDs at $B = 60$ and 84 μT appear visually similar, subtle differences in the distribution of persistent features are reflected in the PH-based indicator discussed below.

To link the extracted topological features to real-space structures, we perform an inverse analysis. Figure 4 presents the inverse analysis[28] for two states at applied OOP magnetic fields $B = 60$ and 108 μT, tracing the specific data points in PD back to the original structure in the real-space configuration. In each state, the points labeled (a), (b), and (c) correspond to data points in the PD with a large lifetime (a), a small lifetime and a small birth value (b), and a small lifetime and a large birth value (c). It is observed that data points with a large lifetime originate from a complex structure, while those with a small lifetime originate from a simple structure, consistent with the simulation data, as described in the supplementary material. The result reflects the distribution of data points in the PDs (Fig. 3), as disordered lattices contain additional microscopic defects, such as dislocations and disclinations, which lead to more complex topological features compared with ordered lattices. Hence, the PH framework effectively links the actual configurational structure of the skyrmion lattice to the features represented in the corresponding PD, which is difficult to capture with the conventional orientational-order measure.

Persistent homology-based indicator and comparison with conventionally used measure of ordering

We then benchmark the PH-based indicator against the conventional orientational order parameter. Figure 5 presents the persistent generator count with relative stability $\langle \tilde{\chi} \rangle$ as a function of $\langle |\Psi_6| \rangle$, along with the first derivatives of both indicators. A positive correlation is observed, as confirmed by the Pearson correlation coefficients $r = 0.993$ and $r = 0.861$ for the values and their derivatives, respectively. These results confirm the consistency between the PH-based indicator and the conventional orientational order parameter. The high sensitivity, in particular the first derivatives, supports the validity of the persistent homology-based approach, as phase transitions are characterized by abrupt, non-analytic changes in system properties.[39] The dependence of $\langle \tilde{\chi} \rangle$ and $\langle |\Psi_6| \rangle$ on the applied OOP field B, together with the details of the Gaussian process regression used to estimate the first derivatives, is provided in the supplementary material and Fig. S7.

For the planar PH construction used here, the computational cost is $O(N \log N)$, which is comparable to that of the conventionally used measure $\langle |\Psi_6| \rangle$. Its practical value, however, lies in providing multiscale and nonlocal structural information beyond nearest-neighbor bond order within a single framework. Obtaining structurally related information by conventional means often requires additional analyses; for example, a straightforward direct evaluation of the orientational correlation function can scale as $O(N^2)$.[40] Accordingly, the proposed indicator remains computationally tractable for large datasets, while still capturing topology-based structural information motivated by topological invariants.[36] More exhaustive topological constructions can become combinatorially expensive;[37] in this sense, the present PH-based indicator offers a practical route to incorporating topological information into lattice-order analysis at a lower computational cost.

The ability of PH analysis to capture ordering may stem from the same geometric foundation as the conventional orientational order parameter, as both rely on the Voronoi tessellation; however, PH further incorporates algebraic topology techniques.[41] One limitation, however, is that the persistent homology-based indicator $\langle\tilde{\chi}\rangle$ may require comparisons across different system states to provide meaningful insights. In contrast, the conventionally used measure of the ordering $\langle|\Psi_6|\rangle$ has a clear physical interpretation due to its normalization, which ensures values between 0 (disordered state) and 1 (perfect hexagonal order).[5] Nevertheless, the PH-based indicator can be further generalized through an entropy-based formulation, as algebraic topology provides a well-defined correspondence with thermodynamic quantities.[26,27] Such a generalization could offer a unified framework for describing both structural complexity and statistical behavior.

CONCLUSION

In this work, we propose a topological indicator, a Persistent Generator Count with Relative Stability (PGCRS) $\langle\tilde{\chi}\rangle$, to characterize phases and phase transitions in two-dimensional quasiparticle systems. As a model system, we use skyrmions, which can be well described as quasiparticles that form lattices in 2D systems. By modeling skyrmions as interacting quasiparticles and applying persistent homology (PH) to their spatial configurations, PGCRS provides a complementary topological descriptor of lattice ordering that remains computationally tractable and is motivated by the stability properties of persistent homology.[35,36] It correlates with the conventional orientational order parameter $\langle|\Psi_6|\rangle$ and reliably traces phase transitions across solid, hexatic, and liquid states. Our analysis demonstrates that the persistence diagram (PD) directly connects the skyrmion configuration to the topological indicator (PGCRS): long-lived features in the PD correspond to disordered, complex configurations, while short-lived ones reflect regular, ordered structures. The applicability of our approach is demonstrated using experimental skyrmion lattices, confirming that the PGCRS produces consistent and reliable phase characterization under realistic experimental conditions. While this work focuses on skyrmion lattice systems, the methodology is broadly applicable to other two-dimensional systems composed of repulsively interacting particles. Future extensions could incorporate insights, such as the Euler entropy, to further strengthen the connection between structural ordering and thermodynamic quantities.[26,27] In summary, PGCRS provides a practical and theoretically grounded framework for efficient, interpretable, and broadly applicable phase analysis in quasiparticle systems.

SUPPLEMENTARY MATERIAL

The supplementary material encompasses the following Supplementary Methods and Supplementary Results: S1. Criteria of Stability Condition for Persistence Diagrams; S2. Conventionally Used Measure of Ordering: Orientational Correlation Function; S3. Gaussian Process Regression; S4. Brownian Dynamics Simulation; S5. Gaussian Process Regression in Experimental Data; S6. Conventional Used Measure of Lattice Ordering in Simulation Data; S7. Persistence Diagrams in Simulation Data; S8. Persistence Diagram Generators and Microscopic Configurations in Simulation Data; S9. Persistent Homology-Based Indicator with Conventional Used Measure of Lattice Ordering in Simulation Data; S10. First Derivatives of Persistent Homology-Based Indicator and Conventionally Used Measure of Ordering in Simulation Data; and S11. Gaussian Process Regression in Simulation Data.

ACKNOWLEDGMENTS

We would like to thank Professor Hans Fangohr for his contributions during the initial phase of this work and for his participation in regular progress discussions. This work was funded by the Deutsche Forschungsgemeinschaft (DFG, German Research Foundation) Project Nos. 403502522 (SPP 2137 Skyrmionics), 49741853, and 268565370 (SFB TRR173 projects A01, B02, and A12) as well as TopDyn, the Zeiss foundation through the Center for Emergent Algorithmic Intelligence, the National Research Council of Science and Technology (NST) grant by the Korean government, MSIT (Grant No. GTL24041-000), the Horizon 2020 Framework Program of the European Commission under FET-Open Grant Agreement No. 863155 (s-Nebula) and ERC-2019-SyG No. 856538 (3D MAGiC), and the Horizon Europe Project No. 101070290 (NIMFEIA).

AUTHOR DECLARATIONS

Conflict of Interest

The authors have no conflicts to disclose.

Author Contributions

M.T. performed the analysis of the simulation and experimental data. J.R. carried out the molecular dynamics simulations. R.G. conducted the Kerr microscopy measurements. T.B.W., C.M., M.K., and M.K. guided and supervised the research. All authors contributed to the interpretation of the results and the writing of the manuscript.

Michiki Taniwaki: Conceptualization (supporting); Data curation (equal); Formal analysis (lead); Investigation (lead); Methodology (lead); Project administration (supporting); Software (lead); Validation (lead); Visualization (lead); Writing – original draft (lead); Writing – review & editing (lead). **Thomas Brian Winkler**: Conceptualization (supporting); Formal analysis (supporting); Investigation (supporting); Methodology (supporting); Project administration (equal); Supervision (lead); Visualization (supporting); Writing – review & editing (lead). **Jan Rothörl**: Data curation (lead); Formal analysis (supporting); Methodology (supporting); Resources (lead); Software (lead); Supervision (equal); Writing – review & editing (lead). **Raphael Gruber**: Data curation (lead); Formal analysis (supporting); Resources (lead); Software (equal). **Chiharu Mitsumata**: Conceptualization (supporting); Formal analysis (supporting); Methodology (supporting); Supervision (lead); Validation (lead); Writing – review & editing (supporting). **Masato Kotsugi**: Funding acquisition (supporting); Resources (equal); Supervision (supporting); Writing – review & editing (supporting). **Mathias Kläui**: Conceptualization (equal); Data curation (supporting); Funding acquisition (lead); Methodology (supporting); Project administration (lead); Resources (lead); Supervision (lead); Validation (supporting); Writing – review & editing (lead).

DATA AVAILABILITY

The experimental and simulation data analyzed in this study are available in the Zenodo repository at https://doi.org/10.5281/zenodo.17801208.

The analysis code used in this study is available in the GitHub repository at https://github.com/MiTaniwaki/PGCRS_2d_quasiparticle.

REFERENCES

[1] S.-G. Je *et al.*, "Direct demonstration of topological stability of magnetic skyrmions via topology manipulation," ACS Nano **14**, 3251–3258 (2020).
[2] K. Everschor-Sitte, J. Masell, R. M. Reeve, and M. Kläui, "Perspective: Magnetic skyrmions—Overview of recent progress in an active research field," J. Appl. Phys. **124**, 240901 (2018).
[3] Y. Ge *et al.*, "Constructing coarse-grained skyrmion potentials from experimental data with iterative Boltzmann inversion," Commun. Phys. **6**, 30 (2023).
[4] S.-Z. Lin, C. Reichhardt, C. D. Batista, and A. Saxena, "Particle model for skyrmions in metallic chiral magnets: Dynamics, pinning, and creep," Phys. Rev. B **87**, 214419 (2013).
[5] J. Zázvorka *et al.*, "Skyrmion lattice phases in thin film multilayer," Adv. Funct. Mater. **30**, 2004037 (2020).
[6] G. Beneke *et al.*, "Gesture recognition with Brownian reservoir computing using geometrically confined skyrmion dynamics," Nat. Commun. **15**, 8103 (2024).
[7] S. Li *et al.*, "Magnetic skyrmions for unconventional computing," Mater. Horiz. **8**, 854–868 (2021).
[8] S. S. P. Parkin, M. Hayashi, and L. Thomas, "Magnetic domain-wall racetrack memory," Science **320**, 190–194 (2008).
[9] R. Msiska, J. Love, J. Mulkers, J. Leliaert, and K. Everschor-Sitte, "Audio classification with skyrmion reservoirs," Adv. Intell. Syst. **5**, 2200388 (2023).
[10] M. Kläui, "Freezing and melting skyrmions in 2D," Nat. Nanotechnol. **15**, 726–727 (2020).
[11] R. Gruber *et al.*, "Real-time observation of topological defect dynamics mediating two-dimensional skyrmion lattice melting," Nat. Nanotechnol. **20**, 1405–1411 (2025).
[12] Y.-W. Li and M. P. Ciamarra, "Accurate determination of the translational correlation function of two-dimensional solids," Phys. Rev. E **100**, 062606 (2019).
[13] P. Huang *et al.*, "Melting of a skyrmion lattice to a skyrmion liquid via a hexatic phase," Nat. Nanotechnol. **15**, 761–767 (2020).
[14] H. Edelsbrunner and J. Harer, "Persistent homology—A survey," Contemp. Math. **453**, 257–282 (2008).
[15] I. Obayashi, T. Nakamura, and Y. Hiraoka, "Persistent homology analysis for materials research and persistent homology software: HomCloud," J. Phys. Soc. Jpn. **91**, 091013 (2022).
[16] I. Donato *et al.*, "Persistent homology analysis of phase transitions," Phys. Rev. E **93**, 052138 (2016).
[17] Y. Hiraoka *et al.*, "Hierarchical structures of amorphous solids characterized by persistent homology," Proc. Natl. Acad. Sci. U. S. A. **113**, 7035–7040 (2016).
[18] P. Bubenik, "Statistical topological data analysis using persistence landscapes," J. Mach. Learn. Res. **16**, 77–102 (2015).
[19] F. Chazal and B. Michel, "An introduction to topological data analysis: Fundamental and practical aspects for data scientists," Front. Artif. Intell. **4**, 667963 (2021).
[20] R. Nagaoka *et al.*, "Quantification of the coercivity factor in soft magnetic materials at different frequencies using topological data analysis," IEEE Trans. Magn. **60**, 4000305 (2024).
[21] S. Kunii, K. Masuzawa, A. L. Fogiatto, C. Mitsumata, and M. Kotsugi, "Causal analysis and visualization of magnetization reversal using feature extended Landau free energy," Sci. Rep. **12**, 19892 (2022).
[22] S. Kunii, A. L. Foggiatto, C. Mitsumata, and M. Kotsugi, "Super-hierarchical and explanatory analysis of magnetization reversal process using topological data analysis," Sci. Technol. Adv. Mater.: Methods **2**, 445–459 (2022).
[23] A. L. Foggiatto, S. Kunii, C. Mitsumata, and M. Kotsugi, "Feature extended energy landscape model for interpreting coercivity mechanism," Commun. Phys. **5**, 277 (2022).
[24] M. Taniwaki *et al.*, "Automated identification of the origin of energy loss in non-oriented electrical steel by feature extended Ginzburg-Landau free-energy framework," Sci. Rep. **15**, 23758 (2025).
[25] M. A. Brems, T. Sparmann, S. M. Fröhlich *et al.*, "Realizing quantitative quasi-particle modeling of skyrmion dynamics in arbitrary potentials," Phys. Rev. Lett. **134**(4), 046701 (2025).
[26] O. Bobrowski and P. Skraba, "Homological percolation and the Euler characteristic," Phys. Rev. E **101**, 032304 (2020).
[27] M. Kastner, "Phase transitions and configuration space topology," Rev. Mod. Phys. **80**, 167–187 (2008).
[28] I. Obayashi, "Stable volumes for persistent homology," J. Appl. Comput. Topol. **7**, 671–706 (2023).
[29] S. C. Kapfer and W. Krauth, "Two-dimensional melting: From liquid-hexatic coexistence to continuous transitions," Phys. Rev. Lett. **114**, 035702 (2015).
[30] R. Gruber, S. M. Fröhlich, J. Rothörl *et al.*, "Skyrmion lattice domain formation in a non-flat energy landscape," Commun. Phys. **9**, 29 (2026).
[31] R. Gruber, J. Rothörl, S. M. Fröhlich *et al.*, "Skyrmion lattice order controlled by confinement geometry," Appl. Phys. Lett. **127**(21), 212403 (2025).
[32] I. Labrie-Boulay *et al.*, "Machine-learning-based detection of spin structures," Phys. Rev. Appl. **21**, 014014 (2024).
[33] H. Edelsbrunner, D. Letscher, and A. Zomorodian, "Topological persistence and simplification," Discrete Comput. Geom. **28**, 511–533 (2002).
[34] A. Zomorodian and G. Carlsson, "Computing persistent homology," Discrete Comput. Geom. **33**, 249–274 (2005).
[35] D. Cohen-Steiner, H. Edelsbrunner, and J. Harer, "Stability of persistence diagrams," Discrete Comput. Geom. **37**, 103–120 (2007).
[36] V. Kurlin, "A one-dimensional homologically persistent skeleton of an unstructured point cloud in any metric space," Comput. Graphics Forum **34**, 253–262 (2015).
[37] N. Otter, M. A. Porter, U. Tillmann, P. Grindrod, and H. A. Harrington, "A roadmap for the computation of persistent homology," EPJ Data Sci. **6**, 17 (2017).
[38] D. Schick *et al.*, "Two levels of topology in skyrmion lattice dynamics," Phys. Rev. Res. **6**, 013097 (2024).
[39] R. J. Gooding and J. R. Morris, "Absence of enhanced fluctuations as a first-order phase transition is approached: An exact transfer-matrix study," Phys. Rev. E **47**, 2934–2937 (1993).
[40] K. Reuter and J. Köfinger, "CADISHI: Fast parallel calculation of particle-pair distance histograms on CPUs and GPUs," Comput. Phys. Commun. **236**, 274–284 (2019).
[41] K. Xia and G.-W. Wei, "Persistent homology analysis of protein structure, flexibility, and folding," Int. J. Numer. Methods Biomed. Eng. **30**, 814–844 (2014).